Chinese Physics Letters

LETTER

Electron–Phonon Coupling with Spin and Orbital Angular Momentum Transfer

Cite as: Mengxiang Xie *et al*. 2026 *Chin. Phys. Lett.* **43** 110703

DOI CSTR

Recommended Articles

Phonon Angular Momentum Generation in Single-Stranded Helix Structure
Hong Sun, Jiaqi Chen, Qingxuan Wang, Xiaoliang Zeng, Jun Zhou, and Lifa Zhang
Chin. Phys. Lett. **42**, 090711 (2025)

First-Principles Study on Thermal and Electrical Transport Properties of $NbGe_2$ and $NbSi_2$: The Role of Electron–Phonon Coupling
Gui-Lin Zhu, Man-Yu Shang, and Jing-Tao Lü
Chin. Phys. Lett. **41**, 126301 (2024)

Electron-Phonon Coupling Drives the Gapless Charge Density Wave in Few-Layer 1T-VSe_2
Yonglong Cheng, Yimanqi He, and Xiangfan Xu
Chin. Phys. Lett. , (2026)

Ultrasmall (3,0) Carbon Nanotube: a Superconducting Unit with Strong Electron–Phonon Coupling
Zhenfeng Ouyang, Jing Jiang, Jian-Feng Zhang, Miao Gao, Kai Liu, and Zhong-Yi Lu
Chin. Phys. Lett. , (2026)

Theoretical prediction of superconductivity and nontrivial band topology in rock-salt transition-metal hydrides *M*H (*M* = Mo, W, Ru, Rh, Y)
Yan-Li Zhang, Hao Ding, Han Wang, Ya-Ping Li, Jin-Han Tan, Na Jiao, Rui Wang, and Hong-Yan Lu
Chin. Phys. Lett. , (2026)

Charge Density Wave Induced Second-Harmonic Generation in 1T-$TaSe_2$
Zhao-Zhe Chen, Chang-Hua Li, Hai-Xia Zhu, Yan-Peng Qi, and Si Xiao
Chin. Phys. Lett. **43**, 080404 (2026)

A series journal of Chinese Physical Society distributed by IOP Publishing

Chinese Physics Letters

Chin. Phys. Lett. **43** 110703 (2026)

LETTER

DOI: 10.1088/0256-307X/43/11/110703
CSTR: 32039.14.0256-307X.43.11.110703

Electron–Phonon Coupling with Spin and Orbital Angular Momentum Transfer

Mengxiang Xie and Jie Ren*

Center for Phononics and Thermal Energy Science, China-EU Joint Lab on Nanophononics, School of Physics Science and Engineering, Tongji University, Shanghai 200092, China

*Corresponding author. Email: xonics@tongji.edu.cn

Spin and orbital angular momentum transfer between lattice vibrations and electrons has become an important focus beyond traditional electron–phonon coupling. Recent studies of spin–rotation coupling have shown that the rotational motion of lattice elastic vibrations can directly interact with the electron spin. Here we develop a microscopic description of the electron–phonon angular momentum coupling beyond spin–rotation coupling, which includes both the electron spin and orbital angular momentum from the relative motion of atoms in a local co-rotating lattice. We relate the lattice angular velocity to the atom-relative angular momentum through the inertia tensor, so that the lattice angular momentum, coupled to total electron angular momentum, contains both phonon spin and orbital angular momentum. The microscopic construction connects with continuum rotation descriptions, extends to non-rigid motion, and reveals discrete-lattice effects beyond the long-wavelength limit. These results provide a microscopic framework of electron–phonon coupling with spin and orbital angular momentum transfer, enabling both studies of phonon-driven electron spin and orbital dynamics and electron-driven phonon spin and orbital dynamics.

Introduction

Electron–phonon interaction plays a fundamental role in material and condensed-matter physics, including charge transport, relaxation, superconductivity, spintronics, quantum information, and so on [1]. How electrons interact with lattice vibrations has been described in many theories, including the Fröhlich-type interaction [2] and piezoelectric coupling [3] in polar materials, in which lattice motion affects electrons through polarized electric fields. For nonpolar scenarios, we have the traditional deformation-potential [4] and Peierls-type coupling [5–8] which describe the influence of lattice stretching or compressive deformation on electron energy and inter-site hopping. This stretching or compressive deformation corresponds to the symmetric part of displacement gradient strain tensor, whose bulk strain (the divergence of the displacement field $\nabla\cdot\boldsymbol{u}$) is locally coupled with the electron without considering spin flipping.

The antisymmetric part of the displacement gradient, $\nabla\times\boldsymbol{u}$, on the other hand, represents a local spatial rotation of lattice vibrations. In this context, the half vorticity $\nabla\times\dot{\boldsymbol{u}}/2$ is assumed to couple the local angular velocity of lattice rotation to the electron spin angular momentum [9–13]. This so-called spin–rotation coupling can be traced back to neutron interferometry in a rotating frame [14–16]. Recently, the generation of electron spin current via lattice motion has attracted growing interest in experiments [17–19], some of which are explicitly attributed to the consequence of spin–rotation coupling, such as in surface acoustic waves in magnetic materials [17]. The similar spin current induced by spin–rotation coupling has also been studied theoretically in bulk waves in chiral materials [20,21].

In addition, spin-current generation has been studied in mechanically rotating systems [22] and differentially rotating systems [23]. Global rigid-body rotation has also been incorporated into treatments of total angular-momentum conservation in magnetic insulators [24], while an independent SO(3) microrotation field has been introduced to describe rotational optical modes in a continuum theory [25]. At the single-ion level, inertial couplings of localized electrons have been derived for circular ionic motion [26]. However, for real crystals with numerous atoms and discrete coordination environments, the rotational motion depends not only on the central atom but also on the relative motion of neighboring atoms. The above methods and descriptions motivate more general microscopic questions: How does the local rotation component couple the electronic angular momentum to the lattice angular momentum? Can we identify this electron–phonon angular momentum coupling (AMC) directly from the atomic motion?

Developments in the study of phonon and elastic-wave angular momentum offer a useful perspective on this problem. Studies of phonon spin date back to early work on transverse phonons in 1961 and 1962 [27–29]. Subsequent work has explored angular momentum associated with circular or elliptical atomic vibrations [30–33], as well as intrinsic spin angular momentum in elastic waves [34–39]. Beyond intrinsic spin, elastic waves also carry orbital angular momentum associated with the spatial structure of the wave field [34,36,40], whose interplay with spin has enabled phonon spin selectivity through elastic spin–orbit interactions [41]. Therefore, we expect that both the spin and orbital angular momentum of phonons should contribute to the electron–phonon AMC.

In this Letter, we develop this angular momentum approach by relating the rotation of the local co-rotating frame to the relative motion of its atomic coordination environment. Our results show that this rotational coupling is naturally related to the atom-relative angular momentum $\boldsymbol{L}$, allowing this interaction to be interpreted as electron–phonon AMC,

$$H_{\mathrm{AMC}}\sim\boldsymbol{L}\cdot\boldsymbol{J}_{\mathrm{e}}, \tag{1}$$

where $\boldsymbol{J}_{\mathrm{e}}=\boldsymbol{s}_{\mathrm{e}}+\boldsymbol{l}_{\mathrm{e}}$ is the total electron angular momentum with $\boldsymbol{s}_{\mathrm{e}}$ and $\boldsymbol{l}_{\mathrm{e}}$ denoting its spin and orbital parts, and the lattice angular momentum $\boldsymbol{L}=\boldsymbol{s}+\boldsymbol{\ell}$ can also be expressed in terms of the summed phonon spin and orbital contributions.

We further examine their relation to the angular vector expansion, identifying how coordination anisotropy affects the orbital and spin contributions to the angular velocity. And the conventional half-vorticity expression is recovered by the leading-order rotation angular velocity under the isotropic condition. We then generalize our results to weak non-rigid distortions by using a best-fit rotation construction method, while a bcc lattice example illustrates finite-wave-vector departures from the continuum prediction. These results provide a basis

Received 24 July 2026; accepted 30 September 2026; published 10 November 2026

© 2026 Chinese Physical Society and IOP Publishing Ltd. All rights, including for text and data mining, AI training, and similar technologies, are reserved.

Check for updates

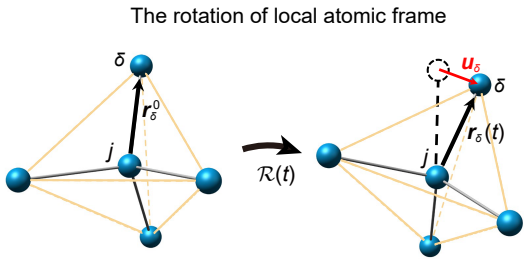

Fig. 1. Rigid rotation of a local coordination environment. The reference bond vectors $\boldsymbol{r}_\delta^0$ and the instantaneous bond vectors $\boldsymbol{r}_\delta(t)$ are related by the same rotation matrix $\mathcal{R}(t)$, $\boldsymbol{r}_\delta(t) = \mathcal{R}(t)\boldsymbol{r}_\delta^0$. The relative displacement is $\boldsymbol{u}_\delta(t) = (\mathcal{R}(t) - \mathbf{1})\boldsymbol{r}_\delta^0$.

for combining discrete lattice dynamics with electronic angular momentum to investigate electron–phonon spin and orbital interactions.

Electron–Phonon Angular Momentum Coupling

We start with a rigidly rotating environment of lattice coordination centered near atom j (see Fig. 1) with an infinitesimal angular vector $\boldsymbol{\theta}(t) = (\theta_x, \theta_y, \theta_z)^{\mathrm{T}}$. To simplify notation, we hold the central atom fixed at the origin of the laboratory frame $\boldsymbol{r}_j(t) = 0$ and $\boldsymbol{r}_\delta(t)$ denotes the instantaneous bond vector connecting the central atom j to a neighboring atom δ. We omit the subscript j in the following derivation and will restore the center index j when summing over different sites in the total Hamiltonian.

The SO(3) rotation is parameterized as $\mathcal{R}(t) = \exp[\boldsymbol{\Theta}(t)]$, where the matrix

$$\boldsymbol{\Theta}(t) = \begin{pmatrix} 0 & -\theta_z & \theta_y \\ \theta_z & 0 & -\theta_x \\ -\theta_y & \theta_x & 0 \end{pmatrix} \tag{2}$$

satisfies $\boldsymbol{\Theta}\boldsymbol{r} = \boldsymbol{\theta}\times\boldsymbol{r}$ for an arbitrary vector $\boldsymbol{r}$, and rotates the initial $\boldsymbol{r}^0$ to $\boldsymbol{r}(t) = \mathcal{R}(t)\boldsymbol{r}^0$. All neighboring bonds under rotation thus satisfy $\boldsymbol{r}_\delta(t) = \mathcal{R}(t)\boldsymbol{r}_\delta^0$, where $\boldsymbol{r}_\delta^0$ is the initial equilibrium bond vector expressed in the local frame. As such, we have

$$\dot{\boldsymbol{r}}_\delta(t) = \dot{\mathcal{R}}\boldsymbol{r}_\delta^0 = \dot{\mathcal{R}}\mathcal{R}^{\mathrm{T}}\boldsymbol{r}_\delta = \boldsymbol{\Omega}\times\boldsymbol{r}_\delta. \tag{3}$$

The instantaneous angular velocity $\boldsymbol{\Omega}$, obtained as

$$\boldsymbol{\Omega} = \dot{\boldsymbol{\theta}} + \frac{1}{2}\boldsymbol{\theta}\times\dot{\boldsymbol{\theta}} + \frac{1}{6}\boldsymbol{\theta}\times(\boldsymbol{\theta}\times\dot{\boldsymbol{\theta}}) + \cdots, \tag{4}$$

is the axial vector of the matrix

$$\dot{\mathcal{R}}\mathcal{R}^{\mathrm{T}} = \dot{\boldsymbol{\Theta}} + \frac{1}{2}[\boldsymbol{\Theta}, \dot{\boldsymbol{\Theta}}] + \frac{1}{6}[\boldsymbol{\Theta}, [\boldsymbol{\Theta}, \dot{\boldsymbol{\Theta}}]] + \cdots, \tag{5}$$

by applying the Baker–Campbell–Hausdorff equality, and $[\boldsymbol{\Theta}, \dot{\boldsymbol{\Theta}}] = (\boldsymbol{\theta}\times\dot{\boldsymbol{\theta}})\times$ when applied to a vector. It is worth noting that the angular velocity $\boldsymbol{\Omega}$ is not simply $\dot{\boldsymbol{\theta}}$, but contains the second- and high-order terms, which represent the non-commutative nature of rotations between different rotation axes.

Now, we consider the rotation associated with the electronic state. On the electron Hilbert space, the spatial rotation (more precisely, its SU(2) lift, since the electrons have spin 1/2) is represented by a unitary operator $\mathcal{U}[\mathcal{R}(t)]$ [42] that connects the electronic state in the local co-rotating frame to that in the laboratory frame through $|\psi_{\mathrm{lab}}\rangle = \mathcal{U}[\mathcal{R}(t)]|\psi_{\mathrm{loc}}\rangle$. Note that for the electron spinor field in four-dimensional Minkowski spacetime, spatial rotations form the SO(3) subgroup of the Lorentz group [43]. The instantaneous rotation is implemented by the unitary operator $\mathcal{U}[\mathcal{R}(t)] = \exp[-(\mathrm{i}/\hbar)\boldsymbol{\theta}\cdot\boldsymbol{J}_{\mathrm{e}}]$, where $\boldsymbol{J}_{\mathrm{e}} = \boldsymbol{s}_{\mathrm{e}} + \boldsymbol{l}_{\mathrm{e}}$ is the total electron angular momentum with $\boldsymbol{s}_{\mathrm{e}}$ and $\boldsymbol{l}_{\mathrm{e}}$ denoting its spin and orbital parts.

Substituting the state relation into the Schrödinger equation $\mathrm{i}\hbar(\partial/\partial t)|\psi_{\mathrm{loc}}\rangle = H_{\mathrm{loc}}|\psi_{\mathrm{loc}}\rangle$, we have

$$\mathrm{i}\hbar\frac{\partial}{\partial t}|\psi_{\mathrm{lab}}\rangle = \mathcal{U}H_{\mathrm{loc}}\mathcal{U}^\dagger|\psi_{\mathrm{lab}}\rangle + H_{\mathrm{AMC}}|\psi_{\mathrm{lab}}\rangle, \tag{6}$$

where the last term $H_{\mathrm{AMC}} := \mathrm{i}\hbar\dot{\mathcal{U}}\mathcal{U}^\dagger$ is the lattice-rotation-induced interaction. The rotation generator and its time derivative generally do not commute, and straightforward calculation leads to

$$\begin{aligned}\dot{\mathcal{U}}\mathcal{U}^\dagger &= \left(\frac{\mathrm{d}}{\mathrm{d}t}\mathrm{e}^{Q(t)}\right)\mathrm{e}^{-Q(t)} \\ &= \dot{Q} + \frac{1}{2}[Q,\dot{Q}] + \frac{1}{6}[Q,[Q,\dot{Q}]] + \cdots,\end{aligned} \tag{7}$$

where $Q = -(\mathrm{i}/\hbar)\boldsymbol{\theta}\cdot\boldsymbol{J}_{\mathrm{e}}$.

Using the angular-momentum commutation relation $[\boldsymbol{J}_{\mathrm{e},\alpha}, \boldsymbol{J}_{\mathrm{e},\beta}] = \mathrm{i}\hbar\epsilon_{\alpha\beta\gamma}\boldsymbol{J}_{\mathrm{e},\gamma}$, we obtain $[Q,\dot{Q}] = -(\mathrm{i}/\hbar)\left(\boldsymbol{\theta}\times\dot{\boldsymbol{\theta}}\right)\cdot\boldsymbol{J}_{\mathrm{e}}$, $[Q,[Q,\dot{Q}]] = -(\mathrm{i}/\hbar)\left[\boldsymbol{\theta}\times(\boldsymbol{\theta}\times\dot{\boldsymbol{\theta}})\right]\cdot\boldsymbol{J}_{\mathrm{e}}$, and so on, which indicates

$$\dot{\mathcal{U}}\mathcal{U}^\dagger = -\frac{\mathrm{i}}{\hbar}\left[\dot{\boldsymbol{\theta}} + \frac{1}{2}\boldsymbol{\theta}\times\dot{\boldsymbol{\theta}} + O(|\theta|^2\dot{\theta})\right]\cdot\boldsymbol{J}_{\mathrm{e}} = -\frac{\mathrm{i}}{\hbar}\boldsymbol{\Omega}\cdot\boldsymbol{J}_{\mathrm{e}}. \tag{8}$$

Therefore, we finally obtain

$$H_{\mathrm{AMC}} := \mathrm{i}\hbar\dot{\mathcal{U}}\mathcal{U}^\dagger = \boldsymbol{\Omega}\cdot\boldsymbol{J}_{\mathrm{e}}, \tag{9}$$

which describes the angular momentum coupling between electrons and phonons under the lattice rotation. As we will discuss in the following sections, $\boldsymbol{\Omega} = \mathcal{I}^{-1}\boldsymbol{L}$ contains contributions from both phonon spin and orbital angular momentum, with $\mathcal{I}$ denoting the inertia tensor.

Microscopic Construction of Angular Velocity

In this section, we would like to show the microscopic construction of angular velocity $\boldsymbol{\Omega}$ by the lattice motion of discrete atoms. Multiplying Eq. (3) by $m_\delta\boldsymbol{r}_\delta\times$ where m_δ is the mass of atom δ and summing over the shell, we have

$$\mathcal{I}\boldsymbol{\Omega}(t) = \boldsymbol{L}, \tag{10}$$

where $\mathcal{I}(t) = \sum_\delta m_\delta\left(|\boldsymbol{r}_\delta|^2\mathbf{1} - \boldsymbol{r}_\delta\boldsymbol{r}_\delta^{\mathrm{T}}\right)$ is the instantaneous inertia tensor of the selected coordination shell for the center atom j, and the total angular momentum $\boldsymbol{L} = \sum_\delta\boldsymbol{L}_\delta = \sum_\delta m_\delta\boldsymbol{r}_\delta\times\dot{\boldsymbol{r}}_\delta$ is the sum of the angular momenta of the neighboring atoms in the coordination shell centered on atom j. As such, the local angular momentum coupling is

$$H_{\mathrm{AMC}} = \mathcal{I}^{-1}\boldsymbol{L}\cdot\boldsymbol{J}_{\mathrm{e}}. \tag{11}$$

Similar to $\boldsymbol{J}_{\mathrm{e}}$ that contains both electron spin and orbital angular momentum, the total lattice angular momentum $\boldsymbol{L} = \mathcal{I}\boldsymbol{\Omega}$ also contains both spin and orbital parts. To make the physical content clearer, we can separate the atomic position $\boldsymbol{r}_\delta(t) = \boldsymbol{r}_\delta^0 + \boldsymbol{u}_\delta(t)$ as the equilibrium position $\boldsymbol{r}_\delta^0$ and displacement vector $\boldsymbol{u}_\delta(t)$. Since $\dot{\boldsymbol{r}}_\delta(t) = \dot{\boldsymbol{u}}_\delta(t)$, the relative angular momentum of each bond separates as

$$\begin{aligned}&\boldsymbol{L}_\delta = m_\delta\boldsymbol{r}_\delta\times\dot{\boldsymbol{r}}_\delta = \boldsymbol{\ell}_\delta + \boldsymbol{s}_\delta, \\ &\boldsymbol{\ell}_\delta = m_\delta\boldsymbol{r}_\delta^0\times\dot{\boldsymbol{u}}_\delta, \quad \boldsymbol{s}_\delta = m_\delta\boldsymbol{u}_\delta\times\dot{\boldsymbol{u}}_\delta,\end{aligned} \tag{12}$$

where $\boldsymbol{\ell}_\delta$ can be regarded as the orbital angular momentum associated with the tilting motion of the equilibrium bond arm (Fig. 2). And $\boldsymbol{s}_\delta$ measures the internal circular or elliptical motion of the relative displacement itself, which can be seen as the spin angular momentum of the relative motion analogous to the spin angular momentum of an elastic displacement field [34,36,40] (Fig. 2).

Summing the bond contributions over the selected coordination shell, we obtain

$$\boldsymbol{\Omega} = \mathcal{I}^{-1}\sum_\delta m_\delta(\boldsymbol{r}_\delta^0\times\dot{\boldsymbol{u}}_\delta + \boldsymbol{u}_\delta\times\dot{\boldsymbol{u}}_\delta) = \mathcal{I}^{-1}(\boldsymbol{\ell} + \boldsymbol{s}), \tag{13}$$

where $\boldsymbol{\ell} = \sum_\delta\boldsymbol{\ell}_\delta$ and $\boldsymbol{s} = \sum_\delta\boldsymbol{s}_\delta$. Substituting Eq. (13) into Eq. (11) and restoring the site index j, we finally arrive at the total AMC Hamiltonian, as

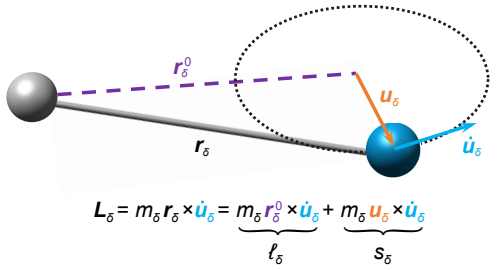

Fig. 2. Geometric decomposition of atom-relative angular momentum. The gray and blue spheres indicate the central atom and instantaneous positions of the neighboring atom, respectively. The bond vector satisfies $\boldsymbol{r}_\delta = \boldsymbol{r}_\delta^0 + \boldsymbol{u}_\delta$. The reference bond $\boldsymbol{r}_\delta^0$ and the relative velocity $\dot{\boldsymbol{u}}_\delta$ define the relative orbital contribution $\boldsymbol{\ell}_\delta = m_\delta \boldsymbol{r}_\delta^0 \times \dot{\boldsymbol{u}}_\delta$. And the elliptical trajectory of the relative displacement illustrates the spin contribution $\boldsymbol{s}_\delta = m_\delta \boldsymbol{u}_\delta \times \dot{\boldsymbol{u}}_\delta$. Their sum gives the complete bond-relative angular momentum, $\boldsymbol{L}_\delta = \boldsymbol{\ell}_\delta + \boldsymbol{s}_\delta$.

$$H_{\mathrm{AMC}} = \sum_j \left[\mathcal{I}_j^{-1}(\boldsymbol{\ell}_j + \boldsymbol{s}_j)\right] \cdot \boldsymbol{J}_{\mathrm{e},j}. \tag{14}$$

Angular Vector Expansion and Continuum Limit

To connect this angular momentum decomposition with the angular vector expansion in Eq. (4), we consider an infinitesimal rigid rotation angular vector $\boldsymbol{\theta}$ of the coordination shell. The displacement can be expressed as $\boldsymbol{u}_\delta = [\mathcal{R}(t) - \mathbf{1}]\boldsymbol{r}_\delta^0 \simeq \boldsymbol{\theta} \times \boldsymbol{r}_\delta^0 + 1/2[\boldsymbol{\theta} \times (\boldsymbol{\theta} \times \boldsymbol{r}_\delta^0)] + O(|\boldsymbol{\theta}|^3)$. Substituting the above displacement and corresponding velocity into Eq. (12) gives

$$\begin{aligned}\boldsymbol{\ell} &= \sum_\delta m_\delta \boldsymbol{r}_\delta^0 \times \dot{\boldsymbol{u}}_\delta \\ &= \mathcal{I}^0 \dot{\boldsymbol{\theta}} + \sum_\delta \frac{m_\delta \boldsymbol{r}_\delta^0}{2} \times \left([\dot{\boldsymbol{\theta}} \times (\boldsymbol{\theta} \times \boldsymbol{r}_\delta^0)] + [\boldsymbol{\theta} \times (\dot{\boldsymbol{\theta}} \times \boldsymbol{r}_\delta^0)]\right) + O(\theta^2 \dot{\theta}) \\ &\simeq \mathcal{I}^0 \dot{\boldsymbol{\theta}} + \frac{1}{2}\left[(\mathcal{K}^0 \boldsymbol{\theta}) \times \dot{\boldsymbol{\theta}} - \boldsymbol{\theta} \times (\mathcal{K}^0 \dot{\boldsymbol{\theta}})\right] + O(\theta^2 \dot{\theta}),\end{aligned} \tag{15}$$

where $\mathcal{I}^0$ is the equilibrium inertia tensor and $\mathcal{K}^0 = \sum_\delta m_\delta \boldsymbol{r}_\delta^0 \boldsymbol{r}_\delta^{0\mathrm{T}}$. This expression shows that the relative orbital angular momentum $\boldsymbol{\ell}$ not only contains the components of $\dot{\boldsymbol{\theta}}$ but also the components of $\left[(\mathcal{K}^0 \boldsymbol{\theta}) \times \dot{\boldsymbol{\theta}} - \boldsymbol{\theta} \times (\mathcal{K}^0 \dot{\boldsymbol{\theta}})\right]$ which is of the same order of $\boldsymbol{\theta} \times \dot{\boldsymbol{\theta}}$. Similarly, the lattice spin contribution is

$$\boldsymbol{s} \simeq \sum_\delta m_\delta (\boldsymbol{\theta} \times \boldsymbol{r}_\delta^0) \times (\dot{\boldsymbol{\theta}} \times \boldsymbol{r}_\delta^0) = \mathcal{K}^0 (\boldsymbol{\theta} \times \dot{\boldsymbol{\theta}}) + O(|\boldsymbol{\theta}|^2 |\dot{\boldsymbol{\theta}}|), \tag{16}$$

which contains the components of $\boldsymbol{\theta} \times \dot{\boldsymbol{\theta}}$ and higher-order terms.

For isotropic reference coordination, $\mathcal{K}^0 = C_0 \mathbf{1}$ and $\mathcal{I}^0 = 2C_0 \mathbf{1}$, these expressions simplify to

$$\begin{aligned}\boldsymbol{\ell} &= \mathcal{I}^0 \dot{\boldsymbol{\theta}} + O(|\boldsymbol{\theta}|^2 |\dot{\boldsymbol{\theta}}|), \\ \boldsymbol{s} &= \frac{1}{2} \mathcal{I}^0 \boldsymbol{\theta} \times \dot{\boldsymbol{\theta}} + O(|\boldsymbol{\theta}|^2 |\dot{\boldsymbol{\theta}}|).\end{aligned} \tag{17}$$

As such, for an isotropic rigidly rotating shell, the lowest order of orbital and spin contributions reproduce the two lowest-order terms in Eq. (4).

We next examine the continuum limit of the discrete construction. To establish a continuum correspondence, suppose that the atomic velocities are sampled from a single smooth field $\boldsymbol{v}(\boldsymbol{r})$ and the atomic bond length to the central atom position is small enough comparing to the continuum picture, so that:

$$\dot{\boldsymbol{u}}_\delta = \boldsymbol{v}(\boldsymbol{r}_\delta^0) - \boldsymbol{v}(0) \simeq (\boldsymbol{r}_\delta^0 \cdot \nabla)\boldsymbol{v}. \tag{18}$$

Hence the orbital angular momentum can be expressed as

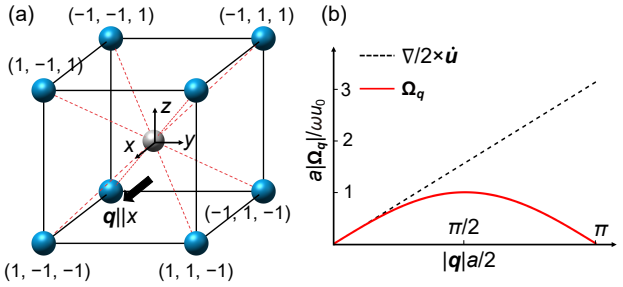

Fig. 3. Discrete rotational response and the long-wavelength limit for a monatomic bcc coordination example. (a) The eight reference nearest-neighbor bonds. The imposed transverse wave has $\boldsymbol{q} = q\boldsymbol{e}_x$ and $\boldsymbol{u}_0 = u_0 \boldsymbol{e}_y$. (b) Angular velocity amplitudes in units of $(\omega u_0)/a$ and plotted against $x = |\boldsymbol{q}|a/2$. The solid red curve is the discrete first-order result, whereas the dashed curve is the continuum half-vorticity reference.

$$\begin{aligned}\boldsymbol{\ell} = \sum_\delta m_\delta \boldsymbol{r}_\delta^0 \times \dot{\boldsymbol{u}}_\delta &\simeq \left[\sum_\delta m_\delta \boldsymbol{r}_\delta^0 (\boldsymbol{r}_\delta^0 \cdot \nabla)\right] \times \boldsymbol{v} \\ &= (\mathcal{K}^0 \nabla) \times \boldsymbol{v},\end{aligned} \tag{19}$$

where the operator $(\mathcal{K}^0 \nabla)_\alpha = \sum_\beta \mathcal{K}^0_{\alpha\beta} \partial_\beta$, $(\alpha, \beta = x, y, z)$ encodes the effect of coordination anisotropy on the rotational response.

Consider the lowest response about the equilibrium configuration, the spin contribution is second order, and the orbital angular momentum yields the lowest nonvanishing (i.e., first-order) angular velocity. By applying an isotropic condition in the long-wavelength limit, with $\mathcal{K}^0 = \sum_\delta m_\delta \boldsymbol{r}_\delta^0 \boldsymbol{r}_\delta^{0\mathrm{T}} = \mathcal{I}^0/2$, we finally obtain

$$(\mathcal{I}^0)^{-1} \boldsymbol{\ell} \simeq \dot{\boldsymbol{\theta}} \simeq \frac{1}{2} \nabla \times \boldsymbol{v}. \tag{20}$$

Thus, the conventional half-vorticity expression is recovered by the leading-order rotation $\dot{\boldsymbol{\theta}}$, which determines the lowest-order lattice orbital angular momentum.

Non-Rigid Rotation Generalization

The identification of coordination rotation with angular momentum established above applies to rigid motion. Specifically, for the general case, we apply an arbitrary $\mathcal{R}' \in \mathrm{SO}(3)$ to fit the local co-rotating frame of Eckart type and obtain the rotation operator $\mathcal{R}$ with the minimum residual deformation [44],

$$\mathcal{R}(t) = \arg\min_{\mathcal{R}' \in \mathrm{SO}(3)} \frac{1}{2} \sum_\delta m_\delta \left| \boldsymbol{r}_\delta(t) - \mathcal{R}' \boldsymbol{r}_\delta^0 \right|^2. \tag{21}$$

The remaining deformation is retained through

$$\begin{aligned}\boldsymbol{r}_\delta &= \mathcal{R}(\boldsymbol{r}_\delta^0 + \boldsymbol{\eta}_\delta), \\ \dot{\boldsymbol{r}}_\delta &= \boldsymbol{\Omega} \times \boldsymbol{r}_\delta + \mathcal{R}\dot{\boldsymbol{\eta}}_\delta.\end{aligned} \tag{22}$$

Here, $\mathcal{R}$ represents the fitted rotation while $\boldsymbol{\eta}_\delta$ describes the residual deformation in the local co-rotating frame. An infinitesimal variation of Eq. (21) gives the stationary condition

$$\sum_\delta m_\delta \boldsymbol{r}_\delta^0 \times \boldsymbol{\eta}_\delta = 0, \quad \sum_\delta m_\delta \boldsymbol{r}_\delta^0 \times \dot{\boldsymbol{\eta}}_\delta = 0. \tag{23}$$

Multiplying the velocity relation in Eq. (22) by $m_\delta \boldsymbol{r}_\delta \times$ and summing yields

$$\begin{aligned}\mathcal{I}(t)\boldsymbol{\Omega} &= \boldsymbol{L} - \mathcal{R}\boldsymbol{\Lambda}, \\ \boldsymbol{\Lambda} &= \sum_\delta m_\delta \boldsymbol{\eta}_\delta \times \dot{\boldsymbol{\eta}}_\delta.\end{aligned} \tag{24}$$

When the residual deformation satisfies $\|\mathcal{I}^{-1}\mathcal{R}\boldsymbol{\Lambda}\| \ll \|\mathcal{I}^{-1}\boldsymbol{L}\|$, the contribution from $\boldsymbol{\Lambda}$ can be treated as a small correction, and we have

$$\boldsymbol{\Omega} \approx \mathcal{I}^{-1}(t)\boldsymbol{L}. \tag{25}$$

BCC Lattice Example

We finally adopt the bcc lattice with lattice constant a to illustrate the rotational response of a discrete atomic lattice. We take the eight nearest-neighbor bonds [Fig. 3(a)]. Expanding the configuration-fitted angular velocity and retaining the lowest order in displacement amplitude gives

$$\boldsymbol{\Omega}_I(t) \simeq \dot{\boldsymbol{\theta}} \simeq (\mathcal{I}^0)^{-1} \sum_\delta m \boldsymbol{r}_\delta^0 \times \dot{\boldsymbol{u}}_\delta(t), \tag{26}$$

where $\mathcal{I}^0 = \sum_\delta m \left(|\boldsymbol{r}_\delta^0|^2 \mathbf{1} - \boldsymbol{r}_\delta^0 \boldsymbol{r}_\delta^{0\mathrm{T}}\right) = 4ma^2\mathbf{1}$ is the equilibrium inertia tensor and $\boldsymbol{r}_\delta^0 = (a/2)(\pm1, \pm1, \pm1)^{\mathrm{T}}$.

Consider a plane-wave displacement sampled at the reference atomic positions, $\boldsymbol{u}_\delta(t) = \mathrm{Re}\left\{\boldsymbol{u}_0[\exp(\mathrm{i}\boldsymbol{q}\cdot\boldsymbol{r}_\delta^0) - 1]\exp(-\mathrm{i}\omega t)\right\}$, where the subtraction $\exp(\mathrm{i}\boldsymbol{q}\cdot\boldsymbol{r}_\delta^0) - 1$ accounts for the displacement relative to the central atom. The corresponding first-order angular velocity is $\boldsymbol{\Omega}_I(t) = \mathrm{Re}\left[\boldsymbol{\Omega}_{\boldsymbol{q}} \exp(-\mathrm{i}\omega t)\right]$, where

$$\boldsymbol{\Omega}_{\boldsymbol{q}} = \frac{\omega}{a}\left[\boldsymbol{f}(\boldsymbol{q}) \times \boldsymbol{u}_0\right], \tag{27}$$

with

$$\boldsymbol{f}(\boldsymbol{q}) = \begin{pmatrix} \sin(q_x a/2)\cos(q_y a/2)\cos(q_z a/2) \\ \cos(q_x a/2)\sin(q_y a/2)\cos(q_z a/2) \\ \cos(q_x a/2)\cos(q_y a/2)\sin(q_z a/2) \end{pmatrix}. \tag{28}$$

In the long-wavelength limit, $\boldsymbol{f}(\boldsymbol{q}) = (a/2)\boldsymbol{q} + O\left[(a|\boldsymbol{q}|)^3\right]$, and hence

$$\boldsymbol{\Omega}_{\boldsymbol{q}} \simeq \frac{\omega}{2}\boldsymbol{q} \times \boldsymbol{u}_0, \tag{29}$$

which reduces to $\nabla/2 \times \dot{\boldsymbol{u}}$ since $\nabla\times \to \mathrm{i}\boldsymbol{q}\times$ and $\partial_t \to -\mathrm{i}\omega$ for the monochromatic wave [See Fig. 3 (b)].

Conclusion

We have established a microscopic angular momentum description of rotational phonon–electron coupling by relating local lattice rotation, which arises from atom-relative motion, to electron angular momentum. For rigid rotation, the angular velocity is determined by the total atom-relative angular momentum via the inertia tensor, thereby linking electronic angular momentum to both the relative orbital and spin contributions of lattice motion.

The small-rotation expansion further clarifies the connection between this angular momentum decomposition and the geometry of rotations. In the long-wavelength limit, this orbital contribution to the angular velocity reduces to half the velocity-field vorticity for isotropic coordination. For non-rigid motion, we adopt a minimum-fitting rotation method to extend the rigid-rotation results. The monatomic bcc example illustrates finite-wave-vector corrections to the continuum limit. Our work provides a microscopic framework for rotation-induced electron–phonon coupling with spin and orbital angular momentum transfer, enabling studies of both phonon-driven electron spin and orbital dynamics and electron-driven phonon spin and orbital dynamics.

Acknowledgments

This work was supported by the National Key R&D Program of China (Grant Nos. 2022YFA1404400 and 2023YFA1406900) and the Opening Project of Shanghai Key Laboratory of Special Artificial Microstructure Materials and Technology.

References

[1] Giustino F 2017 *Rev. Mod. Phys.* **89** 015003
[2] Fröhlich H 1954 *Adv. Phys.* **3** 325
[3] Jhalani V A, Zhou J J, Park J, Dreyer C E, and Bernardi M 2020 *Phys. Rev. Lett.* **125** 136602
[4] Bardeen J and Shockley W 1950 *Phys. Rev.* **80** 72
[5] Vozmediano M A H, Katsnelson M I, and Guinea F 2010 *Phys. Rep.* **496** 109
[6] Sohier T, Calandra M, Park C H, Bonini N, Marzari N, and Mauri F 2014 *Phys. Rev. B* **90** 125414
[7] Suzuura H and Ando T 2002 *Phys. Rev. B* **65** 235412
[8] Su W P, Schrieffer J R, and Heeger A J 1979 *Phys. Rev. Lett.* **42** 1698
[9] Calero C, Chudnovsky E M, and Garanin D A 2005 *Phys. Rev. Lett.* **95** 166603
[10] Chudnovsky E M, Garanin D A, and Schilling R 2005 *Phys. Rev. B* **72** 094426
[11] Matsuo M, Ieda J, and Maekawa S 2013 *Phys. Rev. B* **87** 115301
[12] Matsuo M, Ieda J, Harii K, Saitoh E, and Maekawa S 2013 *Phys. Rev. B* **87** 180402(R)
[13] Xu M, Yamamoto K, Puebla J, Baumgaertl K, Rana B, Miura K, Takahashi H, Grundler D, Maekawa S, and Otani Y 2020 *Sci. Adv.* **6** eabb1724
[14] Mashhoon B 1988 *Phys. Rev. Lett.* **61** 2639
[15] Anandan J 1992 *Phys. Rev. Lett.* **68** 3809
[16] Mashhoon B 1992 *Phys. Rev. Lett.* **68** 3812
[17] Kobayashi D, Yoshikawa T, Matsuo M, Iguchi R, Maekawa S, Saitoh E, and Nozaki Y 2017 *Phys. Rev. Lett.* **119** 077202
[18] Kim K, Vetter E, Yan L *et al.* 2023 *Nat. Mater.* **22** 322
[19] Ohe K, Shishido H, Kato M, Utsumi S, Matsuura H, and Togawa Y 2024 *Phys. Rev. Lett.* **132** 056302
[20] Funato T, Matsuo M, and Kato T 2024 *Phys. Rev. Lett.* **132** 236201
[21] Nishimura N, Funato T, Matsuo M, and Kato T 2025 *J. Magn. Magn. Mater.* **630** 173386
[22] Matsuo M, Ieda J, Saitoh E, and Maekawa S 2011 *Phys. Rev. B* **84** 104410
[23] Funato T, Kinoshita S, Tanahashi N, Nakamura S, and Matsuo M 2025 *Phys. Rev. B* **111** L060403
[24] Rückriegel A, Streib S, Bauer G E W, and Duine R A 2020 *Phys. Rev. B* **101** 104402
[25] Matsuo M, Nishimura N, Yamakage A, and Kato T 2026 arXiv:2605.01678 [cond-mat.mtrl-sci]
[26] Geilhufe R M 2022 *Phys. Rev. Research* **4** L012004
[27] Vonsovskii S V and Svirskii M S 1961 *Fizika Tverdogo Tela* **3** 2160
[28] Vonsovskii S V and Svirskii M S 1962 *Sov. Phys.: Solid State* **3** 1568
[29] Levine A T 1962 *Il Nuovo Cimento* **26** 190
[30] Zhang L and Niu Q 2014 *Phys. Rev. Lett.* **112** 085503
[31] Hamada M, Minamitani E, Hirayama M, and Murakami S 2018 *Phys. Rev. Lett.* **121** 175301
[32] Zhang H, Peshcherenko N, Yang F, Ward T Z, Raghuvanshi P, Lindsay L, Felser C, Zhang Y, Yan J Q, and Miao H 2025 *Nat. Phys.* **21** 1387
[33] Juraschek D M, Geilhufe R M, Zhu H *et al.* 2025 *Nat. Phys.* **21** 1532
[34] Long Y, Ren J, and Chen H 2018 *Proc. Natl. Acad. Sci. U.S.A.* **115** 9951
[35] Yuan W, Yang C, Zhang D, Long Y, Pan Y, Zhong Z, Chen H, Zhao J, and Ren J 2021 *Nat. Commun.* **12** 6954
[36] Ren J 2022 *Chin. Phys. Lett.* **39** 126301
[37] Yang C, Zhang D, Zhao J, Gao W, Yuan W, Long Y, Pan Y, Chen H, Nori F, Bliokh K Y, Zhong Z, and Ren J 2023 *Phys. Rev. Lett.* **131** 136102
[38] Xin S, Xie M, and Ren J 2025 *Chin. Phys. Lett.* **42** 064301
[39] He Y, Luo G, Sohn H, Matsuda O, Wright O B, and Su Z 2026 *Nat. Commun.* **17** 3520
[40] Bliokh K Y 2022 *Phys. Rev. Lett.* **129** 204303
[41] Yang C and Ren J 2024 *Proc. Natl. Acad. Sci. U.S.A.* **121** e2411427121
[42] Messiah A 1999 Quantum Mechanics (Dover Publications, Mineola, NY)
[43] Soper D E 2008 Classical Field Theory (Dover Publications, Mineola, NY)
[44] Szalay V 2017 *J. Chem. Phys.* **146** 124107